A Monte Carlo method for *in silico* modeling and visualization of Waddington's epigenetic landscape with intermediate details

Xiaomeng Zhang[a,c], Ket Hing Chong[a,c], Lin Zhu[b], Jie Zheng[b,*]

[a] *Biomedical Informatics Lab, School of Computer Science and Engineering, Nanyang Technological University, 639798, Singapore*
[b] *School of Information Science and Technology, ShanghaiTech University, Pudong District, Shanghai 201210, China*
[c] *These authors contributed equally to this work.*

Abstract

Waddington's epigenetic landscape is a classic metaphor for describing the cellular dynamics during the development modulated by gene regulation. Quantifying Waddington's epigenetic landscape by mathematical modeling would be useful for understanding the mechanisms of cell fate determination. A few computational methods have been proposed for quantitative modeling of landscape; however, to model and visualize the landscape of a high dimensional gene regulatory system with realistic details is still challenging. Here, we propose a Monte Carlo method for modeling the Waddington's epigenetic landscape of a gene regulatory network (GRN). The method estimates the probability distribution of cellular states by collecting a large number of time-course simulations with random initial conditions. By projecting all the trajectories into a 2-dimensional plane of dimensions i and j, we can approximately calculate the quasi-potential $U(x_i, x_j, *) = -\ln P(x_i, x_j, *)$, where $P(x_i, x_j, *)$ is the estimated probability of an equilibrium steady state or a non-equilibrium state. Compared to the state-of-the-art methods, our Monte Carlo method can quantify the global potential landscape (or emergence behavior) of GRN for a high dimensional system. The potential landscapes show that not only attractors represent stability, but the

*Corresponding author
Email address: zhengjie@shanghaitech.edu.cn (Jie Zheng)

paths between attractors are also part of the stability or robustness of biological systems. We demonstrate the novelty and reliability of our method by plotting the potential landscapes of a few published models of GRN.

Keywords: Waddington's epigenetic landscape; Monte Carlo; gene regulatory network; dynamical systems

1. Introduction

The Waddington's epigenetic landscape has been recognized as a powerful metaphor for explaining the phenomena of embryonic development and cellular differentiation in biology (Waddington, 1957; Goldberg et al., 2007; Slack, 2002; Yamanaka, 2009; Yu et al., 2020). The essence of the conceptual model proposed by Waddington is the ability to explain the emergent properties of cell fate decisions (Jamniczky et al., 2010). At least two types of approaches based on dynamical systems theory for quantifying the Waddington's epigenetic landscape have been used. The first is the discrete formalism of Boolean network modeling (Davila-Velderrain et al., 2015a; Zhou et al., 2014) and the second is continuous modeling in the form of ordinary differential equations (ODEs) (Davila-Velderrain et al., 2015b; Huang, 2009, 2012). This paper is focused on the second approach.

Recently, a few methods for quantifying and plotting Waddington's epigenetic landscape based on gene regulatory networks (GRNs) have been proposed (Bhattacharya et al., 2011; Ferrell Jr, 2012; Li and Wang, 2013; Wang et al., 2011; Zhou et al., 2012). A key step in these methods is the formulation of a potential (or quasi-potential) value for the dynamical system of GRN. For example, Bhattacharya et al. (2011) proposed a method for mapping aligned trajectories of the dynamical system of GRN in ODEs to a "quasi-potential" surface in the x-y phase space. When investigating mathematical models of two important processes in development, cell-fate induction and lateral inhibition (Ferrell Jr, 2012), Ferrell showed that the unique formulation of the potential surface for the lateral inhibition model can produce a pitchfork bifurcation,

which is consistent with Waddington's epigenetic landscape where a ball representing a cell is moving down the hill and then bifurcates into two valleys (i.e. two stable states).

Later, Zhou et al. (2012) proposed a theoretical framework for the decomposition of vector fields which enables the computation of a "quasi-potential function" for multi-attractor systems. Among recent methods for quantifying Waddington's epigenetic landscape is the one proposed by Li and Wang (2013) who used statistical mechanics to quantify the potential landscape through self-consistent mean field approximation. Their formulation of the potential based on the probability distribution of steady states captures the global potential landscape and the global barrier height measured by the "potential difference between the two attractor minimums and the saddle point on landscape" (Li and Wang, 2013). Li and Wang (2013) also used a path integral method to obtain the kinetic paths of transition between attractors. The self-consistent mean field approximation method has been implemented as a part of a software package named "NetLand" by our group to facilitate the drawing of Waddington's epigenetic landscape (Guo et al., 2017).

Although the method proposed by Li and Wang can quantify potential landscapes for high dimensional GRNs, their method has limitation in the lack of realistic details of the landscape. Moreover, the high dimensionality of the GRN as measured by the number of genes poses challenges for modeling, analysis and visualization; for example, the methods proposed by Bhattacharya et al. (2011) and Ferrell Jr (2012) allow two variables only. In this paper we propose a simple Monte Carlo method for quantifying the Waddington's epigenetic landscape of GRNs of more than two genes. Our algorithm projects the time-course trajectories into a 2-dimensional plane of dimensions i and j to calculate the probability distribution and potential $U(x_i, x_j, *) = -\ln P(x_i, x_j, *)$, where $P(x_i, x_j, *)$ is the estimated probability of an equilibrium steady state or a non-equilibrium state. We demonstrate unique features of the proposed method by plotting the landscapes of a few case studies of GRN from two-dimensional to higher dimensional models. In our Monte Carlo method a large number of random initial

conditions drawn from the state space are used to calculate time-series trajectories based on ODEs. The time-series trajectories are then projected into a plane that is divided into grid boxes to estimate the probability distribution and the quasi-potentials of cell states. Surprisingly, such a simple method can capture detailed features of the dynamical system, such as basin of attraction and unstable manifolds connecting two attractors as a kinetic path in the potential landscape.

Testing on a few published models of GRN showed that our Monte Carlo method can successfully quantify global potential landscapes consistent with the state-of-the-art methods. The case studies demonstrate the power of our computational method in uncovering the detailed dynamical behaviors of GRNs that other methods fail to capture. In addition, we have also used the stochastic approach of Chemical Langevin Equation (CLE) to estimate the probability distribution of states by collecting simulated time series. The potential landscape constructed by the stochastic approach turned out to be consistent with the landscape by the deterministic approach. Our analysis indicates that the structure of a GRN (or in other words model interactions) can contribute to the robustness of the attractors to noise. Moreover, we argue that in the Waddington's epigenetic landscape not only the attractors represent stability, but that the paths between attractors characterised by unstable manifolds of saddle point or stable manifolds to attractor also contribute to the stability or robustness of gene regulatory systems for cell fate decision.

2. Methods

In this paper, we propose a Monte Carlo method to quantify the quasi-potential landscape of equilibrium steady states and non-equilibrium states of a GRN. First, we derive the quasi-potential from chemical master equation (CME) using the Monte Carlo method. Instead of solving the CME using the Gillespie's algorithm (also known as the stochastic simulation algorithm) which is computationally costly, we use numerical simulations of ODE mainly because there are

many efficient ODE solvers to obtain time-course trajectories. The Monte Carlo method is used to: (1) generate a large number of random initial conditions that are used for time-course simulations, and (2) estimate probability distribution from time-course trajectories projected into a 2-dimensional plane to quantify the quasi-potential U. A summary of the Monte Carlo method for quantifying Waddington's epigenetic landscape is given in Algorithm 1. Secondly, we discuss how to use stochastic simulations with CLE, which is an improved computation of tau-leaping method for approximate execution of Gillespie's algorithm (Gillespie, 2007). Using the time-course trajectories generated from CLE we can also quantify the Waddington's epigenetic landscape for a GRN. Our method is based on several assumptions, some of which were inherited from previous publications and others extracted from our own empirical observations. For readers' convenience, we list most of the assumptions that we can think of, along with their justifications and references, in Table 1.

2.1. Quantifying Waddington's epigenetic landscape using deterministic ODE models

2.1.1. Derivation of average state probability used in quasi-potential

To derive the quasi-potential for the dynamics of gene expression driving cell state transition, we start from the definition of the CME (Gillespie, 1977; Toral and Colet, 2014)

$$\frac{dP(\mathbf{x},t)}{dt} = \sum_{j=1}^{m} a_j(\mathbf{x}-\boldsymbol{\nu}_j)P(\mathbf{x}-\boldsymbol{\nu}_j,t) - \sum_{j=1}^{m} a_j(\mathbf{x})P(\mathbf{x},t), \tag{1}$$

where $\mathbf{x} = (x_1, x_2, ..., x_n)$ is the state of the system under study (e.g. a GRN), x_i is the copy number of the ith molecular species, n is the number of molecular species, m is the number of reactions, and $P(\mathbf{x}, t)$ is the probability of the system being in state $\mathbf{x}$ at time t. The function $a_j(.)$ defines the propensity function for the jth reaction and $\boldsymbol{\nu}_j$ is the stoichiometric transition vector for the jth reaction. The CME defines the time-evolution of the function $P(\mathbf{x}, t)$ (Gillespie, 1977). The CME can be interpreted as that the flow of the probability

of a system being in state $\mathbf{x}$ at time t is given by the probability of arriving at $\mathbf{x}$ when reaction j occurs, $a_j(\mathbf{x}-\boldsymbol{\nu}_j)P(\mathbf{x}-\boldsymbol{\nu}_j,t)$ subtracted by the probability of the system leaving $\mathbf{x}$ when reaction j fires, $a_j(\mathbf{x})P(\mathbf{x},t)$ (Sunkara, 2009). Summing up all the possible reactions for j from 1 to m gives Eq. (1). For an introduction of CME readers are refer to Higham (2008). From Eq. (1), we can calculate the probability of a cell in state $\mathbf{x}$ at time t

$$P(\mathbf{x},t) \quad = \quad \int \sum_{j=1}^{m} [(a_j(\mathbf{x}-\boldsymbol{\nu}_j)P(\mathbf{x}-\boldsymbol{\nu}_j,t) - a_j(\mathbf{x})P(\mathbf{x},t))]dt + C \quad (2)$$

In theory, when the time t is large, e.g. approaching infinity, the probability $P(\mathbf{x,\ t})$ will approach the steady-state probability P_{ss} (Wang et al., 2008a, 2010). Wang and co-workers (Wang et al., 2008a, 2010) proposed a formulation for the quasi-potential as $U = -\ln\ P_{ss}$. However, to study the dynamics of a biological system we also calculate the average probability of state at $\mathbf{x}$ over the time from 0 to T, as

$$P(\mathbf{x}) = \frac{\int_0^T P(\mathbf{x},t)dt}{T} \quad (3)$$

According to the definition of the quasi-potential U proposed in (Wang et al., 2008b, 2010), we approximate the quasi-potential U by using $P(\mathbf{x})$ from Eq.(3):

$$U = -\ln\ P(\mathbf{x}) \quad (4)$$

2.1.2. Using Monte Carlo simulation to estimate quasi-potential

It is difficult to solve $U = -\ln\ P(\mathbf{x})$ analytically. Thus, we can use a Monte Carlo method to get an approximate solution. Monte Carlo methods use computer simulations with random sampling to approximate the exact solutions (Metropolis and Ulam, 1949). It has been widely used for solving a variety of problems including landscape modeling. For example, two recent works used Monte Carlo simulations to model epigenetic landscape and cell type transitions. Nakagawa and Narikiyo (2010) proposed a minimal modeling of epigenetic landscape based on the fitness of interacting cells. Wang et al. (2014) proposed a

Monte Carlo method based on an ensemble of parameters to simulate the global dynamics of the epigenetic state network. Our Monte Carlo method is different from the above two methods, in that we use a large number of random initial conditions for simulating trajectories and then estimate the probability $P(\mathbf{x})$ by aggregating the trajectories.

First, from Eq. (3) we discretize the formulation from integral into summation:

$$P(\mathbf{x}) = \frac{\sum\limits_{0 \le t_k \le T} P(\mathbf{x}, t) \Delta t_k}{\sum\limits_{0 \le t_k \le T} \Delta t_k} \tag{5}$$

where Δt_k is the increment of time for $P(\mathbf{x}, t)$. Suppose the initial condition is uniformly distributed, and x_i is not larger than X_i, which is a positive integer fixed by a modeler based on the maximum value in the dynamical system. Then the probability averaged over the initial conditions is given by:

$$P(\mathbf{x}, 0) = \begin{cases} \frac{1}{X_1 \cdot X_2 \cdot \ldots \cdot X_n}, & 1 < x_i \le X_i, (i = 1, 2, ..., n) \\ 0, & \text{otherwise} \end{cases} \tag{6}$$

Next, we randomly choose N initial states $\{\mathbf{x}_1(0), \mathbf{x}_2(0), ..., \mathbf{x}_N(0)\}$ which are uniformly distributed in every dimension. Based on these random initial conditions we simulate N trajectories using the Gillespie's algorithm (Gillespie, 1977) which is again a Monte Carlo method. Let us denote the ith trajectory by $S_i = \{\mathbf{x}_i(t_{i,0}), \mathbf{x}_i(t_{i,1}), \mathbf{x}_i(t_{i,2}), ..., \mathbf{x}_i(t_{i,m_i})\}$, where $\mathbf{x}_i(t_{i,m_i})$ is the state at time t_{i,m_i} for the ith trajectory. From these trajectories we can estimate the probability in Eq. (5) as follows:

$$P(\mathbf{x}) = \frac{\sum\limits_{i=1}^{N} \sum\limits_{j=1}^{m_i} [\mathbf{x}_i(t_{i,j}) = \mathbf{x}] \cdot (t_{i,j} - t_{i,j-1})}{\sum\limits_{i=1}^{N} \sum\limits_{j=1}^{m_i} (t_{i,j} - t_{i,j-1})}, \tag{7}$$

where $[A]$ is the Iverson bracket defined by

$$[A] = \begin{cases} 1, & \text{if } A \text{ is true} \\ 0, & \text{otherwise} \end{cases} \tag{8}$$

From this Monte Carlo method we can estimate the probability distribution of the state at $\mathbf{x}$ given by $P(\mathbf{x})$ and then using Eq. (4) we can obtain the quasi-potential U for the dynamical system.

2.1.3. Improving the speed for quasi-potential estimation by using ODEs

Using the Gillespie's algorithm we can simulate the time-evolution trajectories for CME. However, it incurs very high computational cost for simulating every event of the chemical reactions (Li et al., 2008). According to the Gillespie's work (Gillespie, 2001), when the number of molecules present in the biochemical reactions is large the stochastic and deterministic simulation results are almost equivalent with negligible random fluctuations. Assuming that the number of molecules present in the biochemical reactions is large, we use a numerical solution of ODEs to speed up the computation. We also randomly choose N initial conditions $\{\mathbf{x}_1(0), \mathbf{x}_2(0), ..., \mathbf{x}_N(0)\}$ which are uniformly distributed in every dimension. However, these initial conditions are measured in concentration levels of the molecular species. From these random initial conditions we simulate N trajectories.

After numerically solving the ODEs, the output trajectories can be discretized from the continuous time into specific time steps. As such, we can use Eq. (7) to obtain $P(\mathbf{x})$ for calculating the quasi-potential of the dynamical system. The only difference here is that $\mathbf{x}$ is measured in concentration of each molecular species instead of the number of molecules as in the Gillespie's algorithm. We choose to use an ODE solver with a fixed time increment, i.e. Δt is constant. Let us assume the time difference is given by

$$\Delta t = t_{i,j} - t_{i,j-1} \tag{9}$$

Then, substituting Eq. (9) into Eq. (7) and making simplification, we obtain

$$P(\mathbf{x}) = \frac{\sum_{i=1}^{N} \sum_{j=1}^{m_i} [\mathbf{x}_i(t_{i,j}) = \mathbf{x}]}{N \cdot m_i}. \tag{10}$$

With Eq. (10) we have improved the speed for calculating the quasi-potential

value. However, an accurate estimation of $P(\mathbf{x})$ still involves high computational cost due to the large state space of the system. In order to further improve the speed of computation we apply a coarse graining step defined by

$$P(\mathbf{x}) \approx P(\mathbf{x} - \Delta\mathbf{x} \leq \mathbf{x} \leq \mathbf{x} + \Delta\mathbf{x}) = \frac{\sum_{i=1}^{N}\sum_{j=1}^{m_i}[\mathbf{x}_i(t_{i,j}) \subset (\mathbf{x} - \Delta\mathbf{x}, \mathbf{x} + \Delta\mathbf{x})]}{N \cdot m_i}. \tag{11}$$

The coarse graining above is implemented as the division of a 2-D plane into grid boxes.

2.1.4. Plotting landscape

From previous sections we have derived Eq. (7) and Eq. (11) for calculating $P(\mathbf{x})$. However, these equations are for dynamical systems with high-dimensional state spaces. In order to plot the potential landscape in 3 dimensions for human viewers to understand, we need to reduce the dimensions of a system. Many dimensionality reduction methods can be applied. Here, we first propose a simple method of projecting the trajectories into a 2-dimensional plane which is later confirmed by principal component analysis (PCA). By marginalizing out all the variables except for the ith and jth variables, we can obtain the probability distribution of the states in the ith and jth dimensions as

$$P(x_i, x_j, *) = \sum_{s^1}\sum_{s^2}\dots\sum_{s^{i-1}}\sum_{s^{i+1}}\dots\sum_{s^{j-1}}\sum_{s^{j+1}}\dots\sum_{s^n} {}^{P(x_1=s^1, x_2=s^2, \dots, x_{i-1}=s^{i-1}, x_i, x_{i+1}=s^{i+1}, \dots, x_{j-1}=s^{j-1}, x_j, x_{j+1}=s^{j+1}, \dots, x_n=s^n)} \tag{12}$$

Then, we can subtitute Eq. (12) into Eq. (4) to obtain the quasi-potential of a state in two dimensions

$$U(x_i, x_j, *) = -\ln\ P(x_i, x_j, *). \tag{13}$$

With x_i, x_j and $U(x_i, x_j, *)$ as the x, y and z coordinates respectively, we can plot the landscape in 3 dimensions. Since the calculation of $P(x_i, x_j, *)$ includes the time points from t_0 to t_{m_i}, our method can be used to analyze the properties of transient states, rather than being limited to steady states, and thereby can reveal more dynamical details.

Our Monte Carlo method is summarized in Algorithm 1. Essentially, the algorithm collects N simulated time-course trajectories from random initial conditions in the state space. Here, we use a fixed time step of $\Delta t = 0.1$ for numerical simulation, and thereby we can use the number of time points along a trajectory instead of the length of continuous time to estimate the probability of a state. Then from these time-course data, we project the points of the trajectories into a phase plane of two selected variables of interest and estimate the probabilities of states. For example, Figure 1 shows how the probability values can be estimated in a plane that has been divided into grid boxes. A grid box with a locally maximal number of points on the trajectories represents an attractor. In Figure 1 there are two yellow grid boxes with locally maximal numbers of points on the trajectories, and therefore they represent two attractors. These results are then used to estimate the quasi-potential $U(x_i, x_j, *) = -\ln P(x_i, x_j, *)$. Compared with other methods (e.g. Li and Wang (2013)) our method includes both equilibrium state and non-equilibrium states. A non-equilibrium state quantifies the transient behaviors of the system such as the intermediate flows in a vector field, whereas an equilibrium state quantifies a repeller (unstable steady state) or an attractor (stable steady state) (Tyson et al., 2001). This formulation and approximate calculation of the quasi-potential enables us to plot the Waddington's epigenetic landscape with details.

Algorithm 1. Monte Carlo steps for quantifying quasi-potential landscape

1. generate N random initial conditions
2. select 2 marker genes (proteins) and split the 2-dimensional plane into grid boxes
3. for each initial condition:
   (i) generate one trajectory
   (ii) project the trajectory to the 2-dimensional grid boxes
   (iii) from the trajectory calculate the number of points in each grid box
4. estimate probability of each grid box $P(x_i, x_j, *)$ as given by Eq. (12)

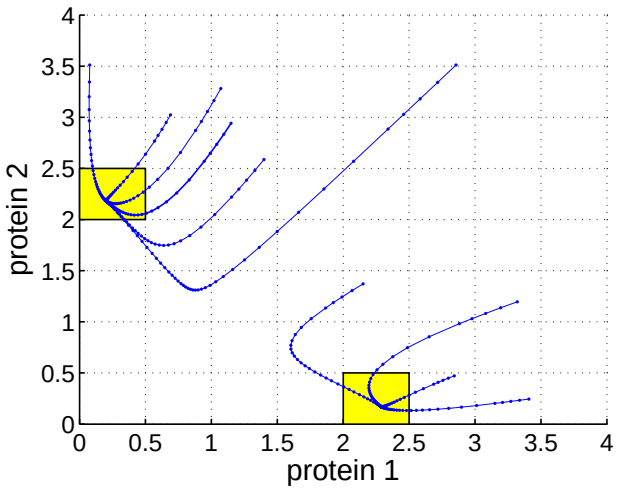

Figure 1: Illustration of the Monte Carlo method for approximating the probability distribution and identifying attractors. The projection of the time-course data into a plane with grid boxes enables the estimation of the probabilities of cellular states. In this example 10 trajectories (blue lines) are shown and the plane is split into 8 x 8 grid boxes. A grid box with a locally maximal number of points of trajectories corresponds to an attractor. In this landscape, there are two attractors as indicated by the two yellow boxes.

5. calculate quasi-potential of each grid box using $U(x_i, x_j, *) = -\ln P(x_i, x_j, *)$
6. plot the landscape in 3 dimensions

2.2. Stochastic modeling of landscape based on Chemical Langevin Equation (CLE)

To test the role of noise in gene expression and the robustness of GRNs we also investigate a second type of potential landscape that is based on stochastic time-course simulations. The algorithm for obtaining the potential landscape is similar to Algorithm 1. The key difference is that the stochastic approach uses Chemical Langevin Equation (CLE) (Gillespie, 2000), an improved version of the tau-leaping method for approximation of the Gillespie's algorithm (Gillespie, 2007), in simulating the time-series trajectories. CLE differs from ODEs in that the biochemical reactions are simulated using the stochastic part in the CLE (Higham, 2008). We adapted the CLE code from Higham (2008) with

the model reactions from the GRNs of Li and Wang (2015) and Gardner et al. (2000). We used a larger noise than in the original code of Higham (2008), by decreasing the volume of the system from $V = 10^{-15}$ to $V = 10^{-20}$. Since CLE is a well-established method for stochastic simulation of biochemical reactions (Gillespie, 2007) we will not discuss it in detail here. The CLE models and their implementation in MATLAB code are given in Supplementary materials. Below we will illustrate how to construct CLE by converting from ODEs. The definitions of the rates of change of molecular species are different between ODEs and CLE. In ODEs the molecular species are measured in concentration, whereas in CLE the molecular species are measured in the number of molecules. To explain how to convert the deterministic rate constant k_i in ODEs to the stochastic reaction rate constant c_i in CLE, let us look at Eq. (16), an example ODE model equation for protein x with self-activation (the first term on the right hand side) and spontaneous degradation (the second term):

$$\frac{dx}{dt} = k_1 \frac{x^n}{k_2^n + x^n} - k_3 x. \tag{14}$$

Let us use X to denote the copy number of protein x. Hereafter we will use the same symbol x to denote the concentration of protein x, in the unit of μM. The relationship between x and X is given by:

$$X = x \cdot N_A \cdot V, \tag{15}$$

where N_A is the Avogadro's number which equals 6.023×10^{23} and V is the volume of the system in liters (Higham, 2008). Next, denote $B = N_A \cdot V$, then Eq. (15) becomes

$$X = x \cdot B.$$

Multiply B to both sides of Eq. (14), and we get

$$\frac{dx}{dt} B = B \cdot k_1 \frac{x^n}{k_2^n + x^n} - k_3 x \cdot B,$$

$$\frac{dx}{dt} B = B \cdot k_1 \frac{B^n \cdot x^n}{B^n (k_2^n + x^n)} - k_3 x \cdot B,$$

$$\frac{d(x \cdot B)}{dt} = B \cdot k_1 \frac{(x \cdot B)^n}{(Bk_2)^n + (x \cdot B)^n} - k_3(x \cdot B).$$

Since $X = x \cdot B$, we obtain the following equation:

$$\frac{dX}{dt} = B \cdot k_1 \frac{(X)^n}{(Bk_2)^n + (X)^n} - k_3 X. \tag{16}$$

In the stochastic approach the rate of change for X is defined by:

$$\frac{\Delta X}{\Delta t} = c_1 \frac{X^n}{c_2^n + X^n} - c_3 \cdot X. \tag{17}$$

Comparing Eq. (18) and Eq. (19), we deduce that,

$$c_1 = B \cdot k_1 = N_A \cdot V \cdot k_1,$$

$$c_2 = B \cdot k_2 = N_A \cdot V \cdot k_2,$$

$$c_3 = k_3$$

From the derivations above, we demonstrate the relationship between k_i and c_i which enables us to obtain the c_i for the stochastic simulation using CLE.

3. Results

3.1. Quantifying the potential landscape of non-equilibrium and equilibrium states

To demonstrate the capability of the proposed method, we selected three GRN models: (1) a bistable synthetic toggle switch (Gardner et al., 2000), (2) a model of cancer attractors (Li and Wang, 2015) and (3) a stem cell differentiation and reprogramming model (Li and Wang, 2013). For the model equations, readers may refer to the original papers or the source code included in our MATLAB package (see the Additional material). These case studies illustrate that our method can capture distinct details of dynamical systems, e.g. attractor, repeller, unstable manifold and saddle point. Furthermore, we compare our method with another constructing landscape method (based on the NetLand (Guo et al., 2017)) from computing costs and results.

3.1.1. Case Study 1: Bistable synthetic toggle switch from Gardner et al. (2000)

In the first case study, our method is used to analyse the transient properties of a synthetic genetic toggle switch proposed by Gardner et al. (2000). The model equations and parameter values we used are the same as given by Segel and Edelstein-Keshet (2013). By applying the Monte Carlo method which is presented as Algorithm 1 in this paper (see Methods), we obtained the landscape as shown in Figure 2A. The potential landscape shows two attractors and there is a valley (or kinetic path) connecting the two attractors. Between the two attractors, there is a saddle point (Figure 2B & 2C).

In Figure 2D phase plane analysis shows that the system displays two attractors and one saddle point. A saddle point is formed by both stable and unstable manifolds (Gardner et al., 2000; Segel and Edelstein-Keshet, 2013; Chong et al., 2015). By comparing the potential landscape with the phase plane (Figure 2D), the valley (or kinetic path) in Figure 2A is found to be formed by the unstable manifolds of saddle point or stable manifolds, which cannot be generated by analysing steady states only.

This simple model of GRN shows that our method of formulating the potential can capture some transient properties of a dynamical system. For example, when there is a valley between two attractors in the potential landscape, the kinetic path is formed by unstable manifolds. The saddle point sets a threshold for the barrier height that can separate the two attractors. The potential landscape displays a three-dimensional view of the phase plane and shows the attractors and saddle point more clearly than a two-dimensional plane. In particular, the saddle point is shown to have one convex (local minimum) and one concave down (local maximum) in the nearly orthogonal directions. The result from this example suggests that not only attractors represent stability but the kinetic paths are also part of the stability of GRNs.

3.1.2. Case Study 2: Cancer attractors from Li and Wang (2015)

To test if our method can handle a network of more than two genes, we choose a six-gene network model proposed by Li and Wang (2015). This gene

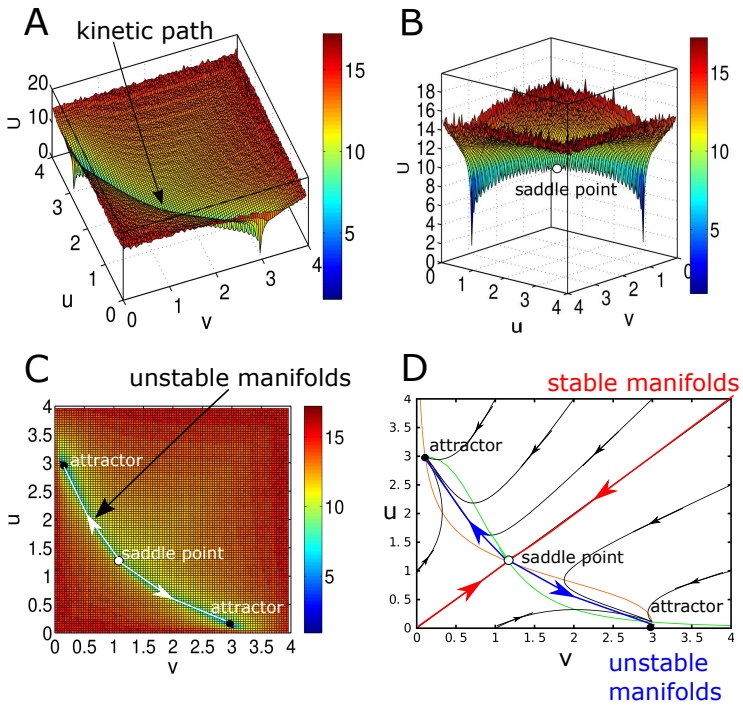

Figure 2: **Potential landscape for Case Study 1. (A)** 3D view of a genetic toggle switch-based landscape: The landscape displays two attractors that are connected with a kinetic path formed by unstable manifolds. **(B)** Side view of the genetic toggle switch-based landscape in Case 1: The landscape displays two basins of attraction that are connected by the unstable manifolds. Separating the two attractors, the saddle point is a tipping point (or barrier height) for transition along the kinetic path between the basins of attraction. **(C)** Top view indicates the kinetic path formed by unstable manifolds. **(D)** Phase plane plot shows the unstable manifolds (blue arrows) from the saddle point form the kinetic path.

network was reported to produce four attractors representing cancer stem cells, stem cells, cancer cells and normal cells (Li and Wang, 2015). The potential landscape of this model generated by our algorithm, however, shows four pairs of attractors in which the two attractors in each pair are close to each other (Figure 3). Our analysis of the end points of the trajectories confirmed that there are 8 attractors (data not shown). The result implicates that Li and Wang (2015) may have joined the two nearby attractors into one attractor and thus resulted in only four attractors.

This result indicates that the potential landscape obtained using our method can capture more details of attractors. In addition, the landscape also contains 6 valleys (Figure 3). These valleys are formed by unstable manifolds, as discussed in the first example, and contain the information about saddle points as barrier heights for separating two attractors. These valleys are similar to the kinetic paths in Case Study 1 in illustrating the transition from one attractor to another attractor in the landscape.

To visualize the Waddington's epigenetic landscape of a gene regulatory network of more than two genes in three dimensions using dimensionality reduction is a problem that we will explore next. We tested the Monte Carlo method with PCA (principal component analysis) where all the trajectories were arranged vertically as each column represents a gene (or a protein) to form a feature matrix and then apply PCA to obtain the two principal components that were later used as the x-axis and y-axis. The Waddington's epigenetic landscape obtained from the Monte Carlo method with PCA is given in Figure 4. The landscape plotted with the first two principal components has preserved the information from the original data. It displays 8 attractors and the landscape is consistent in the number of attractors with that in Figure 3. This result demonstrates that the Monte Carlo method with PCA enables us to plot Waddington's epigenetic landscape in three dimensions without having to select two marker genes and marginalize out all other genes.

3.1.3. Case Study 3: Stem cell differentiation and reprogramming from Li and Wang (2013)

Finally, to test if our method can model high-dimensional gene regulatory networks, we selected a 52-gene network model proposed by Li and Wang (2013) for quantifying the stem cell differentiation and reprogramming. Li and Wang (2013) identified two attractors in the state space of gene expression: stem cell attractor and differentiated cell attractor. To plot the potential landscape we chose two marker genes GATA6 and NANOG as in Li and Wang (2013), which play pivotal roles in regulating stem cell fates, and used their expression levels

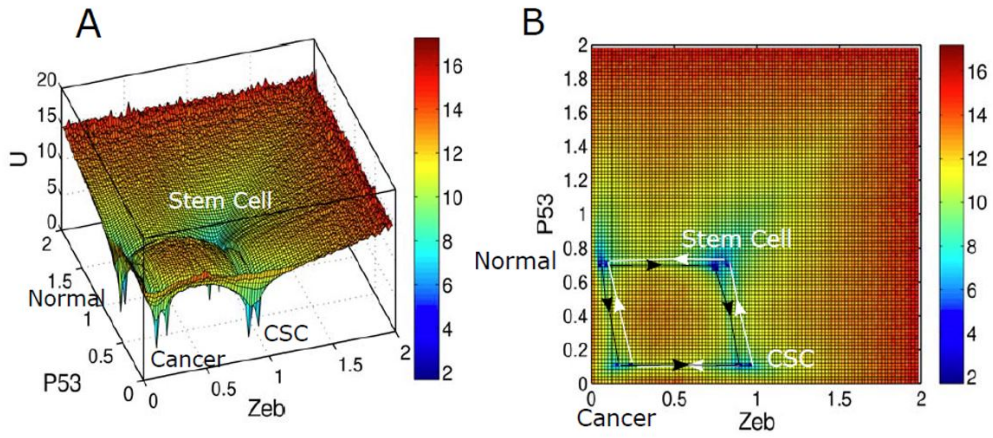

Figure 3: **Potential landscape for Case Study 2. (A)** 3D view of the landscape. Validation of our method by reproducing the potential landscape of Li and Wang (2015) in Case 2. By comparing the locations of the attractors labeled by Li and Wang (2015), we identified the attractors and their corresponding cell states. The landscape displays four main basins of attraction for normal cells, cancer cells, stem cells and cancer stem cells. However, our landscape is slightly different from that in the original paper (Li and Wang, 2015): each of the main basins of attraction is divided into two attractors which are connected by kinetic paths. **(B)** Top view of the landscape. These kinetic paths and their directions are plotted according to Li and Wang (2015). These kinetic paths suggest that cell changes state according to different directions of the kinetic paths (Li and Wang, 2015). The color corresponds to the value of the quasi-potential U.

as the coordinates of the 2D panel. The shape of our potential landscape is consistent with that in Li and Wang (2013), e.g. both showing two attractors (Figure 5). The potential landscape shows that the stem cell attractor has a bigger basin of attraction and lower potential value than the differentiated cell attractor.

The result in Figure 5 suggests that our method can capture the transient non-equilibrium states and the attractors of the equilibrium steady states with more details than the results reported by Li and Wang (2013). The potential landscape displays one dominant attractor shown as the stem cell attractor, which implies that the probability of getting attracted to this stem cell attractor

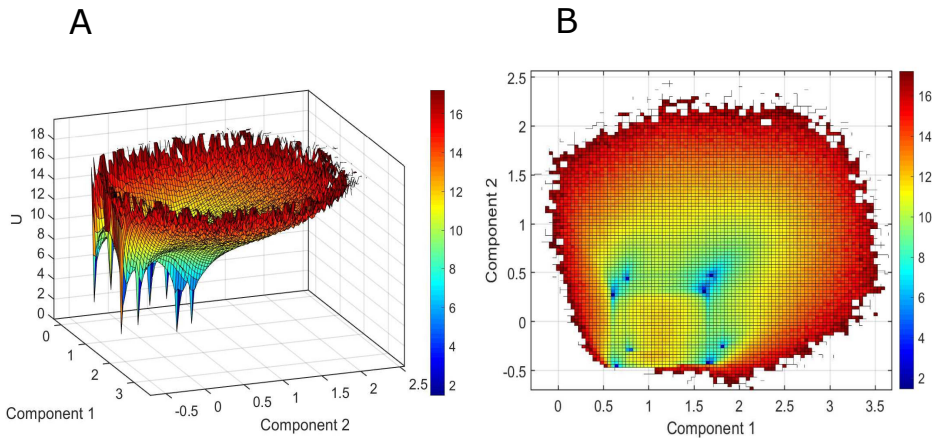

394 Figure 4: **Potential landscape for Case Study 2 plotted using the Monte Carlo**
395 **method with PCA. (A)** 3D view of the Waddington's epigenetic landscape plotted based
396 on the first two principal components. The landscape indicates there are eight attractors
397 which is consistent with the potential landscape obtained using the two selected genes P53
398 and ZEB as shown in Figure 3. **(B)** Top view of the landscape.

418 is higher than the differentiated cell attractor. As with Case Study 2 we also use
419 PCA to plot a potential landscape in three dimensions based on the first two
420 principal components as the coordinates of the 2D panel, as shown in Figure
421 6. Again, PCA has preserved the presence and locations of two attractors as in
422 Figure 5. Moreover, it suggests that the proposed Monte Carlo method can be
423 used to visualize Waddington's epigenetic landscape for high-dimensional gene
424 regulatory networks.

438 *3.1.4. Comparison of our Monte-Carlo method with NetLand*

439 To assess the reliability and advantages of our Monte Carlo method, we com-
440 pare it with NetLand, a state-of-the-art software tool for landscape modeling
441 and visualization (Guo et al., 2017). First, we test and compare the compu-
442 tational efficiency between the two methods. They were tested on the ODE
443 models of the three case studies, running on a ThinkPad Laptop, with Intel
444 Core i7-5500U (CPU 2.4GHz) and memory size of 12GB. As shown in Table 2,
445 our method is faster than NetLand, but needs more memory. Note that NetLand

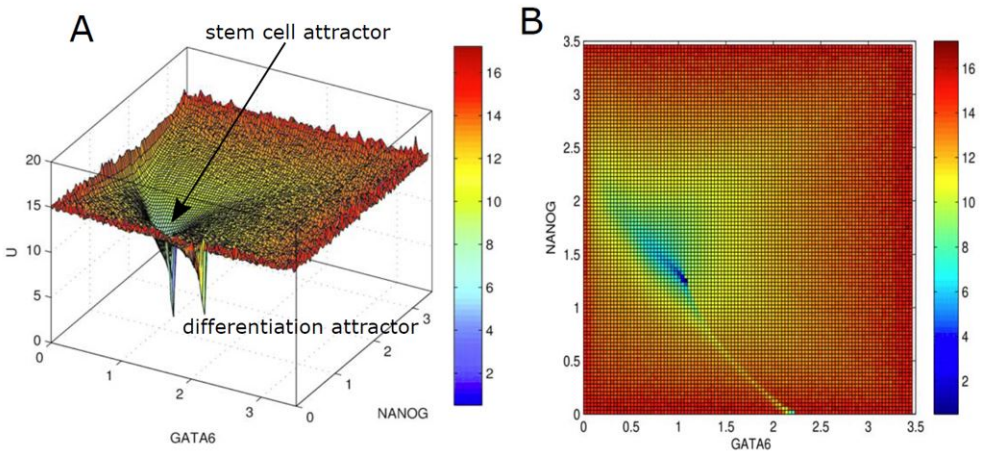

Figure 5: **Potential landscapes for Case Study 3.** **(A)** 3D view of the Waddington's epigenetic landscape based on a 52-gene network model (Li and Wang, 2013), which shows two basins of attraction. By comparing the locations of the attractors labeled by Li and Wang (2013), we observe that the stem cell attractor located on the left is the dominant attractor, i.e. bigger and deeper (blue color) than the differentiation attractor located on the right. **(B)** Top view of the landscape.

is implemented in Java, whereas our Monte Carlo method is in MATLAB. Thus, it is likely that our method can be more efficient when it is re-implemented in another computer language in the future. From the constructed landscape results (as shown in Figure 3 and Figure 7), both methods can capture the steady states of the system. Furthermore, our method can spontaneously reveal kinetic paths between attractors. By contrast, in the output of NetLand, the shape of a basin of attraction is round likely due to the Gaussian approximation and the kinetic paths need to be calculated separately, which has not been implemented in NetLand. Figure 7 is a screenshot of the output of NetLand on Case Study 2. Although the numerical results of NetLand show that there are 8 attractors, it is difficult to find more than 4 attractors in the landscape plot. This example demonstrates the advantage of showing more intermediate details offered by our Monte Carlo method.

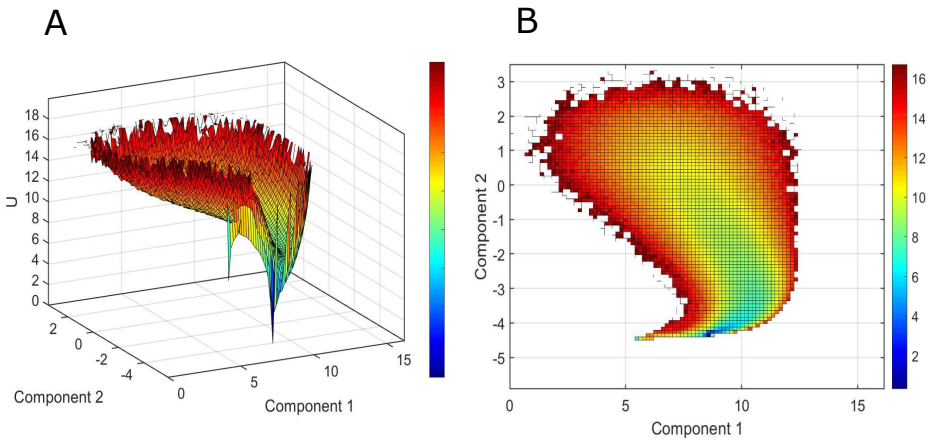

Figure 6: **Potential landscape for Case Study 3 plotted using PCA. (A)** 3D view of the Waddington's epigenetic landscape plotted based on the first two principal components. The landscape shows there are two attractors which is consistent with the potential landscape obtained using the two selected genes GATA6 and NANOG as shown in Figure 5. This landscape is plotted with 60,000 trajectories with random initial conditions due to memory limitation, whereas other landscapes in this paper were plotted with 100,000 trajectories. **(B)** Top view of the landscape.

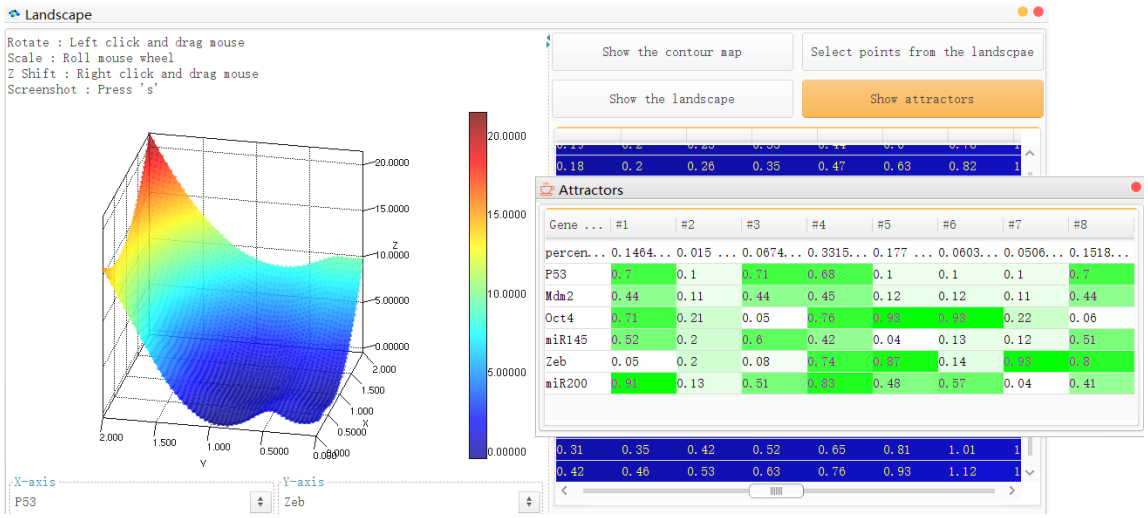

Figure 7: A screenshot of output of NetLand on Cast Study 2 (Li and Wang, 2015).

3.2. Stochastic modeling of landscape based on Chemical Langevin Equation (CLE)

The models of Waddington's epigenetic landscape in the previous section were constructed based on deterministic simulations using ODEs. Here, we also investigate the landscape model for Li and Wang (2015) constructed using a stochastic approach based on Chemical Langevin Equation (CLE) (Gillespie, 2000; Higham, 2008). We applied the same procedure as described in Algorithm 1 in the Methods section with the only difference that the numerical simulation of the time-course data was done with CLE instead of ODEs. For the 6-gene network model in Case Study 2 from Li and Wang (2015), we defined 22 reactions (16 network interactions of activation and inhibition plus 6 self-degradations) and converted the rate constants from the deterministic k_i in ODEs to the stochastic rate constants c_i, as explained in Methods. We simulated 100,000 trajectories with random initial conditions. Two runs of the time-course simulation using CLE with random initial conditions are given in Figure 8A. Each trajectory is projected to a 2D plane of dimensions i and j to estimate the marginalized probability $P(x_i, x_j, *)$ and the quasi-potential $U(x_i, x_j, *) = -\ln P(x_i, x_j, *)$ as in the ODE model. A potential landscape for the model of Li and Wang (2015) obtained from CLE is shown in Figure 8B, which is comparable to the one obtained using deterministic ODE-based simulation (Figure 3A). The stochastic noise in the CLE only slightly perturbed the dynamic simulations as the shapes of the attractors in the potential landscape were almost unchanged (even when we used a larger noise than in the original code of Higham (2008) by changing the volume of the system from $V = 10^{-15}$ to $V = 10^{-20}$). However, the attractors in the potential landscape from CLE display slightly larger basins of attraction. As a result, two of the attractors that are located close to each other in the ODE-based landscape have been merged into one in the CLE-based landscape (Figure 8B). We also set the volume of the system $V = 10^{-15}$ to obtain a large number of molecules, and the landscapes plotted based on ODE and CLE are almost identical (data not shown). The computational time for generating the potential landscape using the CLE is 57.9 minutes, which is much

longer than using the ODEs (12 minutes). This is expected as the stochastic simulation normally takes a longer time due to the high computational cost for simulating all the events of biochemical reactions (Li et al., 2008).

We also performed stochastic simulations using the synthetic toggle switch model of Gardner et al. (2000) and we obtained similar results, i.e. the potential landscape is not affected by the noise (Supplementary Figure S9). These results implicate some degree of robustness of GRNs.

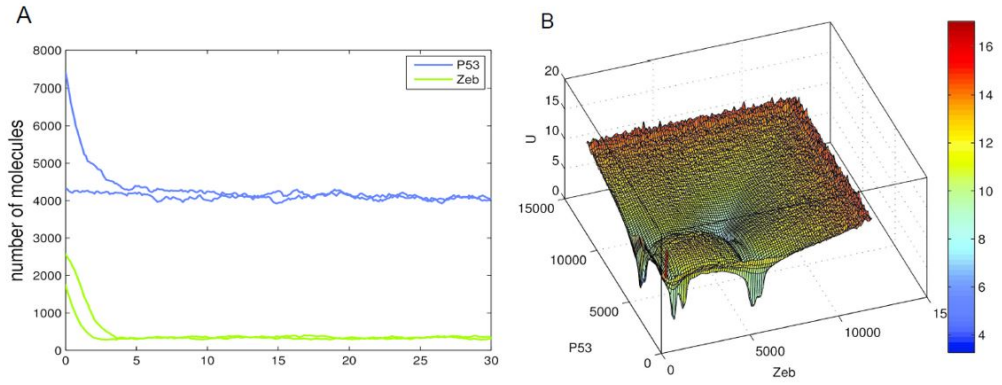

Figure 8: **(A)** Two realizations of time-course simulation of the 6-gene network in Case Study 2 generated from Chemical Langevin Equation (CLE) with random initial conditions. These time-course simulations show that, starting from two different initial conditions, two trajectories with some randomness can eventually converge to the same attractor. **(B)** Waddington's epigenetic landscape of the 6-gene network model from Li and Wang (2015), which shows four basins of attraction. The potential landscape was generated by using CLE-based dynamic simulations, and its shape is consistent with that of the landscape obtained using ODEs shown in Figure 3. It implicates that the attractors in the potential landscape are robust to noise.

4. Discussion

In this paper, we present a simple Monte Carlo method for quantitatively modeling and visualization of Waddington's epigenetic landscape based on dynamical simulation of GRNs. This method uses a large number of initial conditions randomly sampled from a uniform distribution in the state space, and

the collected time-series data are then used to estimate the probability values and the quasi-potential values of cell states in the landscape. One key advantage of our method is that it can quantify the potential landscape to display both global and local dynamics of the cell state transitions for both equilibrium states (e.g. steady states or attractor states) and non-equilibrium states (e.g. transient states along a kinetic path). Dimensionality reduction is an important part of landscape plotting in three dimensions (just as GPLVM used in NetLand (Guo et al., 2017), but it is not a trivial task. We used PCA to plot Waddington's landscapes by using the first two principal components as the coordinates of state space, for Case Study 2 in Figure 4 and for Case Study 3 in Figure 6. The potential landscape from the first two principal components shows a consistent picture of the potential landscape using the two selected genes of P53 and ZEB as shown in Figure 3, e.g. both landscapes show that there are 8 attractors. However, choosing marker genes according to prior biological knowledge can have more interpretability than using dimensionality reduction. Our results suggest that not using dimensionality reduction will often not affect the 3D view of Waddington's epigenetic landscape, since choosing the right pair of genes as the x- and y-axes we could plot a meaningful landscape. Particularly, how genes for x- and y-axes should be chosen are based on key biomarkers in the biological system that contribute to cell fate decisions or cell states as commonly practiced by modelers (Bhattacharya et al., 2011; Li and Wang, 2013; Huang, 2012; Li and Wang, 2015). The landscape provides a 3D view of the dynamical features (e.g. attractor, saddle point, unstable manifold and stable manifold) of the system, whereas conventional dynamical system analysis uses 2D views such as bifurcation diagram, phase plane and vector field. Thus, our computational method can be used for detailed modeling and 3D visualization of dynamical systems of cells.

While the method proposed by Li and Wang (2013) formulates the potential as $U = -\ln P_{ss}$ (where P_{ss} is the steady state probability) and uses the self-consistent mean field approximation, our method uses the estimated probability of any state, either an equilibrium steady state or non-equilibrium tran-

sient states). Li and Wang (2013) also used 100,000 time-course simulations from random initial conditions in the state space and inferred the steady state probability distribution with multi-variable Gaussian distribution to plot the potential landscape, which displays a smooth surface with basins of attraction. Between their method and ours, the locations of attractors are essentially the same. However, our method can capture more detailed information than their method (Li and Wang, 2013, 2015), as demonstrated in Case 2 (with four pairs of attractors as shown in Figure 3) and in Case Study 3 (with one dominant attractor as shown in Figure 5). In Case Study 2, the four pairs of attractors (Figure 3) can be explained by the kinetic paths for the transition between attractors. As for Case Study 3, we are not aware of any biological reason for the landscape to display one dominant stem cell attractor and one minor differentiated cell attractor (Figure 5), which should be investigated in the future. Moreover, our Monte Carlo method is powerful in that it can capture the kinetic path without using the path integral method as in Li and Wang (2013). The kinetic paths proposed by Li and Wang (2013) or the epigenetic valleys as in Ashwin and Sasai (2015) are barrier pathways that describe the intermediate states and the differentiated states. The kinetic path (or valley) between two attractors can give biological insight into the transition from one attractor to another where the intermediate state transitions must follow this path towards the final stable state. The kinetic path in the Waddington's epigenetic landscape can explain why the cell differentiation in embryonic development follows a deterministic path (Waddington, 1957; Lanctôt, 2015) which was called by Waddington himself as "chreod" (Slack, 2002; Jaeger and Monk, 2014).

The potential landscape modeling based on stochastic simulations of Langevin dynamics has also been conducted by Li and Wang (2013). Also, to plot 3D views of landscape, they used the method of root mean square distance (RMSD), i.e. using coordinates of two attractors (with locally minimum potentials) as two reference points to reduce a multi-dimensional space into two dimensions of RMSD1 and RMSD2. Using the Langevin dynamics and RMSD they obtained a landscape with the same number of attractors as the landscape based on their

self-consistent mean field approximation method. However, the topographies of the two landscapes (i.e. from self-consistent mean field approximation and Langevin dynamics with RMSD) reported by Li and Wang Li and Wang (2013) are different. Here, we used Chemical Langevin Equation to obtain the time-course trajectories and applied our Monte Carlo method to directly obtain a landscape. Using the stochastic approach of CLE we can obtain a Waddington's epigenetic landscape consistent with that using the deterministic approach of ODEs. These results of computer simulation highlight the robustness of the gene regulatory network to noise (Wang et al., 2008b; Thattai and Van Oudenaarden, 2001).

5. Conclusion

The Monte Carlo method for plotting potential landscapes for multi-dimensional GRNs allows us to study the links between genotype and phenotype as initially proposed by Conrad Waddington over 60 years ago (Waddington, 1957; Goldberg et al., 2007). Through studies of real biological networks, we demonstrated the simplicity and power of the method for plotting Waddington's epigenetic landscape. It can facilitate our understanding of cellular dynamics, e.g. the differentiation and reprogramming of stem cells as well as other biological processes. In general, the algorithm proposed here for cellular dynamics can also be applied to studying other types of dynamical systems such as social networks.

Acknowledgments

The authors would like to thank Chunhe Li and Sudin Bhattacharya for answering our questions regarding their published methods. We also thank Bard Ermentrout for the permission to use the XPPAUT software for plotting the phase plane.

Availability of data and materials

All the data and materials are provided in the additional files.

Additional files

available at `https://github.com/MCLand-NTU/Zhang_et_al_Supplementary_Information/`

Additional file 1: Supplementary Information

This contains supplementary methods and instructions on how to use the MATLAB code provided to simulate and visualize the Waddington's epigenetic landscapes presented in this paper.

Additional file 2: Supplementary Code.

This file contains the source code in MATLAB format for the implementation of the algorithm used to plot the Waddington's epigenetic landscapes.

Competing interests

The authors declare that they have no competing interests.

Funding

This work was supported by the MOE AcRF Tier 1 grant (2015-T1-002-094), MOE AcRF Tier 1 Seed Grant on Complexity (RGC 2/13, M4011101.020), and MOE AcRF Tier 2 Grant (ARC39/13, MOE2013-T2-1-079), Ministry of Education Singapore, and the start-up grant of ShanghaiTech University, Shanghai, China.

Author's contributions

XZ and KHC designed the method and implemented the algorithm and case studies. LZ contributed in the implementation and test of PCA. JZ supervised the design of the method and the study. XZ, KHC and JZ wrote the manuscript.

References

Ashwin, S., Sasai, M., 2015. Effects of collective histone state dynamics on epigenetic landscape and kinetics of cell reprogramming. Scientific reports 5, 16746.

Bhattacharya, S., Zhang, Q., Andersen, M.E., 2011. A deterministic map of waddington's epigenetic landscape for cell fate specification. BMC Syst. Biol 5, 85.

Chong, K.H., Samarasinghe, S., Kulasiri, D., Zheng, J., 2015. Computational techniques in mathematical modelling of biological switches, in: Weber, T., McPhee, M., Anderssen, R.S. (Eds.), 21st International Congress on Modelling and Simulation (MODSIM 2015), p. 578.

Davila-Velderrain, J., Juarez-Ramiro, L., Martinez-Garcia, J.C., Alvarez-Buylla, E.R., 2015a. Methods for characterizing the epigenetic attractors landscape associated with boolean gene regulatory networks. arXiv preprint arXiv:1510.04230 .

Davila-Velderrain, J., Martinez-Garcia, J.C., Alvarez-Buylla, E.R., 2015b. Modeling the epigenetic attractors landscape: toward a post-genomic mechanistic understanding of development. Front. Genet 6, 160.

Ferrell Jr, J.E., 2012. Bistability, bifurcations, and waddington's epigenetic landscape. Curr. Biol. 22, R458–R466.

Gardner, T.S., Cantor, C.R., Collins, J.J., 2000. Construction of a genetic toggle switch in *Escherichia coli*. Nature 403, 339.

Gillespie, D.T., 1977. Exact stochastic simulation of coupled chemical reactions. J. Phys. Chem. 81, 2340–2361.

Gillespie, D.T., 2000. The chemical langevin equation. J. Chem. Phys. 113, 297–306.

Gillespie, D.T., 2001. Approximate accelerated stochastic simulation of chemically reacting systems. The Journal of chemical physics 115, 1716–1733.

Gillespie, D.T., 2007. Stochastic simulation of chemical kinetics. Annu. Rev. Phys. Chem. 58, 35–55.

Goldberg, A.D., Allis, C.D., Bernstein, E., 2007. Epigenetics: a landscape takes shape. Cell 128, 635–638.

Guo, J., Lin, F., Zhang, X., Tanavde, V., Zheng, J., 2017. Netland: quantitative modeling and visualization of waddington's epigenetic landscape using probabilistic potential. Bioinformatics 33, 1583–1585.

Higham, D.J., 2008. Modeling and simulating chemical reactions. SIAM review 50, 347–368.

Huang, S., 2009. Reprogramming cell fates: reconciling rarity with robustness. Bioessays 31, 546–560.

Huang, S., 2012. The molecular and mathematical basis of waddington's epigenetic landscape: A framework for post-darwinian biology? Bioessays 34, 149–157.

Jaeger, J., Monk, N., 2014. Bioattractors: dynamical systems theory and the evolution of regulatory processes. J. Physiol. 592, 2267–2281.

Jamniczky, H.A., Boughner, J.C., Rolian, C., Gonzalez, P.N., Powell, C.D., Schmidt, E.J., Parsons, T.E., Bookstein, F.L., Hallgrímsson, B., 2010. Rediscovering waddington in the post-genomic age. Bioessays 32, 553–558.

Lanctôt, C., 2015. Single cell analysis reveals concomitant transcription of pluripotent and lineage markers during the early steps of differentiation of embryonic stem cells. Stem Cells 33, 2949–2960.

Li, C., Wang, J., 2013. Quantifying cell fate decisions for differentiation and reprogramming of a human stem cell network: landscape and biological paths. PLOS Comput. Biol 9, e1003165.

Li, C., Wang, J., 2015. Quantifying the landscape for development and cancer from a core cancer stem cell circuit. Cancer Res. 75, 2607–2618.

Li, H., Cao, Y., Petzold, L.R., Gillespie, D.T., 2008. Algorithms and software for stochastic simulation of biochemical reacting systems. Biotechnol. Prog. 24, 56–61.

Metropolis, N., Ulam, S., 1949. The Monte Carlo method. J. Am. Stat. Assoc 44, 335–341.

Nakagawa, M., Narikiyo, O., 2010. Epigenetic landscape of interacting cells: A model simulation for developmental process. Biosystems 101, 156–161.

Segel, L.A., Edelstein-Keshet, L., 2013. A Primer in Mathematical Models in Biology. Siam.

Slack, J.M., 2002. Conrad Hal Waddington: the last renaissance biologist? Nat. Rev. Genet. 3, 889.

Sunkara, V., 2009. The chemical master equation with respect to reaction counts, in: Proc. 18th World IMACS/MODSIM Congress, pp. 703–707.

Thattai, M., Van Oudenaarden, A., 2001. Intrinsic noise in gene regulatory networks. Proc. Natl. Acad. Sci. U.S.A. 98, 8614–8619.

Toral, R., Colet, P., 2014. Stochastic numerical methods: an introduction for students and scientists. John Wiley & Sons.

Tyson, J.J., Chen, K., Novak, B., 2001. Network dynamics and cell physiology. Nat. Rev. Mol. Cell Biol. 2, 908.

Waddington, C., 1957. The strategy of the genes.

Wang, J., Xu, L., Wang, E., 2008a. Potential landscape and flux framework of nonequilibrium networks: Robustness, dissipation, and coherence of biochemical oscillations. Proc. Natl. Acad. Sci. U.S.A. 105, 12271–12276.

699 Wang, J., Xu, L., Wang, E., 2008b. Robustness, dissipations and coherence of
700 the oscillation of circadian clock: potential landscape and flux perspectives.
701 PMC Biophys 1, 7.

702 Wang, J., Xu, L., Wang, E., Huang, S., 2010. The potential landscape of genetic
703 circuits imposes the arrow of time in stem cell differentiation. Biophys. J. 99,
704 29–39.

705 Wang, J., Zhang, K., Xu, L., Wang, E., 2011. Quantifying the waddington
706 landscape and biological paths for development and differentiation. Proc.
707 Natl. Acad. Sci. U.S.A. 108, 8257–8262.

708 Wang, P., Song, C., Zhang, H., Wu, Z., Tian, X.J., Xing, J., 2014. Epigenetic
709 state network approach for describing cell phenotypic transitions. Interface
710 focus 4, 20130068.

711 Yamanaka, S., 2009. Elite and stochastic models for induced pluripotent stem
712 cell generation. Nature 460, 49.

713 Yu, C., Liu, Q., Chen, C., Wang, J., 2020. Quantification of the underly-
714 ing mechanisms and relationship among cancer, metastasis and differentia-
715 tion/development. Front. Genet. 10.

716 Zhou, J.X., Aliyu, M.D.S., Aurell, E., Huang, S., 2012. Quasi-potential land-
717 scape in complex multi-stable systems. J. Royal Soc. Interface 9, 3539–3553.

718 Zhou, J.X., Qiu, X., Fouquier d'Hérouël, A., Huang, S., 2014. Discrete gene
719 network models for understanding multicellularity and cell reprogramming:
720 from network structure to attractor landscape, in: Kriete, A., Eils, R. (Eds.),
721 Computational Systems Biology. Elsevier.

Table 1: A list of assumptions used in our method.

No.	Assumption	Justification	References
1.	100,000 uniform distribution for initial conditions.	We used the uniform distribution for the initial conditions, because we try to avoid any prior bias about initial states of trajectories in the epigenetic landscape. As such, we sample the initial cellular states from the interval of the minimum to maximum gene expression values uniformly, to cover all possible trajectories as completely as possible. The convergence of trajectories to attractors should be driven by the self-organization of GRN, rather than initial conditions. We believe that setting the number of trajectories to 100,000 would be appropriate. Our experiments showed that, with fewer trajectories, the landscape shape will be almost the same, whereas simulating more trajectories won't change the landscape shape very much, although more costly computationally.	Li and Wang (2013)
2.	When the number of molecules present in the biochemical reactions is large the stochastic and deterministic simulation results are almost equivalent.	According to the works of Daniel T. Gillespie, when the populations of reactant molecules are large, any noticeable change of the propensity function in a stochastic model would involve a large number of reaction events. In other words, if this condition is satisfied, then the effect of stochastic variability involving only a few molecules is negligible. As such, stochastic simulations can be approximated by deterministic simulations with high accuracy.	Gillespie (1977, 2001)
3.	The definition of the quasi-potential landscape U is given by the negative of probability distribution of state, $U = -lnP(x)$.	This is a fundamental assumption based on analogy between molecular kinetics such as for cell fate regulation and statistical physics. The idea, definition and formulation of the quasi-potential stem from dynamical systems theory and statistical physics.	Wang et al. (2008b, 2010)
4.	The probability distribution of state P(x) can be estimated with a coarse-grained method based on the division of a 2-D plane into grid boxes.	The cellular process of transcription is also discretized (with bursting) rather than continuous. Also, there are intrinsic and extrinsic noises affecting the cell state transitions. Therefore, the coarse-graining based on division of 2-D plane into grid boxes won't bring much bias or error to the probability estimation.	N.A.

Table 2: Comparison of our Monte Carlo method with NetLand. We compare them from three aspects, including run time, peak memory usage, and the number of detected attractors.

Case studies		Monte Carlo method	NetLand
(Gardner et al., 2000)	Run time (s)	34	33
	Memory usage (GB)	4.5	4.0
	No. of attractors	2	2
(Li and Wang, 2015)	Run time (s)	32	58
	Memory usage (GB)	4.6	4.3
	No. of attractors	8	8
(Li and Wang, 2013)	Run time (s)	90	622
	Memory usage (GB)	5.6	4.6
	No. of attractors	2	2